POLISH MARITIME RESEARCH 4 (120) 2023 Vol. 30; pp. 102-109
10.2478/pomr-2023-0063

# EXPLORATION OF A MODEL THERMOACOUSTIC TURBOGENERATOR WITH A BIDIRECTIONAL TURBINE

**Volodymyr Korobko** [1]
**Serhiy Serbin** [1] *
**Huu Cuong Le** [2]
[1] Admiral Makarov National University of Shipbuilding, Mykolaiv, Ukraine
[2] Institute of Maritime, Ho Chi Minh City University of Transport, Viet Nam

* Corresponding author: *serbin1958@gmail.com (Serhiy Serbin)*

**ABSTRACT**

*The utilisation of the thermal emissions of modern ship power plants requires the development and implementation of essentially new methods of using low-temperature waste heat. Thermoacoustic technologies are able to effectively use low-temperature and cryogenic heat resources with a potential difference of 500–111 K. Thermoacoustic heat machines (TAHMs) are characterised by high reliability, simplicity and environmental safety. The wide implementation of thermoacoustic energy-saving systems is hampered by the low specific power and the difficulties of directly producing mechanical work. An efficient approach to converting acoustic energy into mechanical work entails the utilisation of axial pulse bidirectional turbines within thermoacoustic heat engines. These thermoacoustic turbogenerators represent comprehensive systems that consist of thermoacoustic primary movers with an electric generator actuated by an axial-pulse bidirectional turbine. The development of such a thermoacoustic turbogenerator requires several fundamental issues to be solved. For this purpose, a suitable experimental setup and a 3D computational fluid dynamics (CFD) model of a thermoacoustic engine (TAE) with bidirectional turbines were created. The research program involved conducting physical experiments and the CFD modelling of processes in a TAE resonator with an installed bidirectional turbine. The boundary and initial conditions for CFD calculations were based on empirical data. The adequacy of the developed numerical model was substantiated by the results of physical experiments. The CFD results showed that the most significant energy losses in bidirectional turbines are manifested in the output grid of the turbine.*

**Keywords:** waste heat recovery; ship power plant; thermoacoustics; thermoacoustic engine; bidirectional turbine

## INTRODUCTION

Maritime transport is an important component of the global economy, as it provides the bulk of freight traffic. Marine heat engines consume carbon-based recoverable fuel, producing significant amounts of heat emissions of various potentials that harm the environment. These emissions include fuel combustion products, such as $CO_2$, $SO_n$, $NO_x$, volatile organic compounds (VOCs), carbon particles, etc.

The International Maritime Organization (IMO), in accordance with the provisions of the United Nations Sustainable Development Goal (SDG) 13 [1]–[3], introduced requirements that direct the general trend in shipping towards a significant limitation of the volume and composition of emissions from ship power plants, including diesel and gas turbine units [4]–[8].

The task of the decarbonisation of marine energy has become vital; it aims to minimise the consumption of carbon fuels, which is a key factor in reducing greenhouse gas (GHG)

emissions. The result of these measures was the introduction of efficient dual-fuel engines that use new types of fuel, including cryogenic fuels. These measures led to a significant decrease in the temperature of thermal emissions (Table 1).

Under such conditions, traditional ship thermal emission utilisation schemes, based on the classic water Rankine cycle (WRC), become ineffective. It is these circumstances that lead to the use of other energy-saving technologies, such as the organic Rankine cycle (ORC) system [9] ]–[11] and thermo-chemical conversion [12].

A promising method for the utilisation of the low-temperature thermal emissions of ship power plants (SPPs) may be the use of thermoacoustic technologies [13], [14].

There are two types of thermoacoustic machines: thermoacoustic engines (TAEs) and thermoacoustic refrigerators (TARs), or heat pumps. Thermoacoustic engines (movers) implement a direct process – converting thermal energy from external sources into an acoustic form. A TAR performs the opposite process – it consumes acoustic energy and converts it into the heat with different potential.

*Tab. 1. Temperatures of waste heat carriers of modern SPPs*

| Heat carrier/source | 2S ICE | 4C ICE | PEM FC |
|---|---|---|---|
| | Temperature, K | | |
| Waste gases of ICE | 490–530 | 500–690 | – |
| Air charger | 400–490 | 380–470 | – |
| Cooling system liquid | 355–360 | 360–370 | (LT PEM) 333–363<br>(HT PEM) 450–493 |
| LNG fuel | 111 | 111 | 111 |
| $NH_3$ fuel | 240 | 240 | 240 |

In ship power systems, TAEs can utilise high-potential heat sources with temperatures ranging from 330–550 K or higher, such as emissions from internal combustion engines (ICEs) or electrochemical generators like solid oxide fuel cells (SOFCs) and polymer electrolyte membrane fuel cells (PEMFCs). On the other hand, low-potential thermal sources might be the ambient environment or cryogenic fluids such as liquefied hydrogen ($LH_2$), natural gas (LNG) or ammonia ($NH_3$), with temperatures from 4–240 K [15]. The widespread application of thermoacoustic systems in practice is hindered by the complexity of the efficient conversion of acoustic energy into mechanical work, a low specific power density and the lack of practical experience. Issues related to the development of low-temperature thermoacoustic systems were considered in [16].

In terms of renewable energy, we are familiar with wave power plants that utilise oscillating water columns (OWCs), which incorporate bidirectional turbines like the Wells turbine and impulse bidirectional turbines [17]–[19]. The application of bidirectional turbines in thermoacoustic heat recovery systems has also been addressed in previous studies [19]–[23].

Bidirectional turbines are the most efficient transducers for ship thermoacoustic waste heat recovery systems (WHRSs) when it comes to generating mechanical work and driving electric generators. They are capable of transforming the energy of acoustic oscillation into the rotational motion of the turbine rotor. Therefore, it can be considered that such thermoacoustic turbine generators (TATGs) are the most rational solution for low-temperature ship WHRSs.

Obviously, the use of bidirectional turbines in thermoacoustic devices is an appropriate solution. However, it should be noted that OWC units differ significantly from TAE units in terms of the design and parameters of the working environment, and therefore the direct use of existing approaches in the design of such turbines is problematic. The existing problem is a complex task and requires a set of additional studies.

## FUNCTIONING CONDITIONS OF BIDIRECTIONAL TURBINES

It is known that OWC plants are open systems that operate at atmospheric pressure ($P_m = P_{amb}$). In these systems, the working medium, air, undergoes oscillatory motion. In the flowing part of the OWC, the amplitude of these oscillations' motion can reach several metres, while the frequency of oscillations does not exceed 0.2 to 1 Hz:

$$\zeta = \frac{u_s}{\rho a} = \frac{(0.05–0.1)P_m}{2\pi f\rho\sqrt{\chi RT}}, \quad (1)$$

where $\rho$ is the density of the medium in kg/m$^3$; $\chi$ is the adiabatic index; $T$ is the temperature in K; and $R$ is the universal gas constant.

TAEs are closed systems in which noble gases are the working fluid, the internal pressure $P_m$ can reach 0.3–3.0 MPa and the frequency of the acoustic wave is $f$ = 50–150 Hz.

Accordingly, in thermoacoustic devices, the amplitude of the oscillatory motion of the acoustic wave $\zeta_{TAE}$ is much smaller than $\zeta_{OWC}$(Fig. 1).

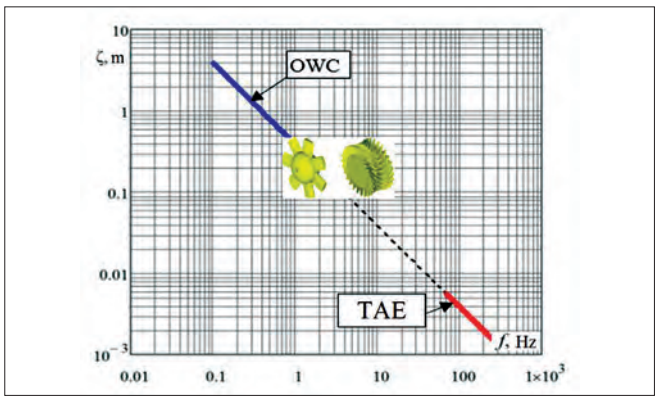


*Fig. 1. Comparison of the amplitudes of the oscillatory motion of the medium in an OWC and a TAE*

It is obvious that the hydrodynamic processes in the flow channels of OWC systems are significantly different from the processes in TAE resonators. In a thermoacoustic apparatus under high-frequency oscillations, the influence of inertial factors on the hydrodynamic parameters of the medium should increase significantly. In addition, there is a significant difference between the designs of the flow parts of these bidirectional turbines. In the case of an OWC, large-volume collectors are used. In thermoacoustic devices, the resonators have much

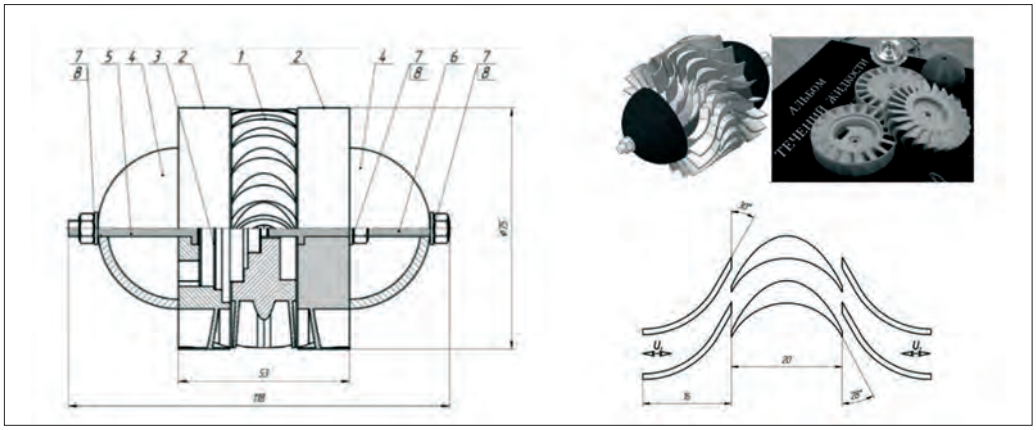

*Fig. 2. Experimental turbine generator assembly: 1 – turbine rotor, 2 – stator, 3 – generator, 4 – fairing, 5 and 6 – turbine axes, 7 and 8 – fasteners*

smaller dimensions. In this regard, it is possible to expect the formation of stable oscillating structures in the TATG resonator, which will introduce additional excitations and inhomogeneities at the input to the rectifier of the turbine. They will create a novel energy-consuming mechanism that should be confined on both sides of the bidirectional turbine. In view of these circumstances, it can be considered appropriate to conduct a complex of studies to obtain an in-depth understanding of these issues.

***Purpose of research.*** Considering the disparities in the working processes between OWCs and TAEs, it is sensible to carry out research focused on understanding the peculiarities of hydrodynamic processes within the TATG resonator to identify the most rational design solutions. Research should involve both physical experiments and numerical calculations using computational fluid dynamics (CFD) procedures, which requires the creation of appropriate equipment and methods of research.

## EXPERIMENTAL SETUP

The investigation was conducted utilising an experimental bidirectional turbine. This turbine was designed and manufactured in accordance with the guidelines outlined in [24]. A 3D model of an experimental bidirectional turbine was developed in the CAD software developed by SolidWorks. The turbine's components, including the rotor, guide grids and fairings, were produced using 3D printing techniques and plastic material, as depicted in Fig. 2. Detailed information about the dimensions of the elements of the experimental bidirectional turbine is provided in Table 2.

The rotor of the turbine was rigidly coupled to a three-phase brushless electric generator of the Sankyo F2JGL type. The output voltage from the generator was fed to a diode converter made of Schottky diodes, and a P517-M laboratory rheostat or a set of precision resistors was used as a load.

The rotation speed of the turbine was monitored by an SDS 1074CFL digital oscilloscope, which was connected to one of the windings of the generator.

Such a scheme made it possible to simultaneously control the speed of rotation of the turbine rotor, the root-mean-square (RMS) voltage of the generator $V_{RMS}$ and the current in the electric grid. The characteristics of bidirectional turbines in a unidirectional flow were studied using the experimental installation, the scheme of which is shown in Fig. 3.

*Tab. 2. Design parameters of bidirectional turbines*

| Element | Value |
|---|---|
| Internal diameter of TAE resonator, mm | 46 |
| Outer diameter of turbine stator, mm | 76 |
| Outer blade diameter of turbine, mm | 75 |
| Turbine rotor diameter, mm | 50 |
| Blade width of rotor, mm | 20 |
| Number of rotor blades | 24 |
| Width of stator blades, mm | 16 |
| Number of stator blades | 18 |

Differential thermostabilised pressure sensors of MPXV NXP semiconductors were used to measure the pressure drop along the turbine and on the entrance lemniscate. The equipment of the experimental stands and the available microprocessor-based data acquisition system (DAS) provided multiple measurements of sensor readings in each of the modes, which reduced the random error.

The STM32F407VGT6 microcontroller, which has a 32-bit architecture and an operating frequency of 168 MHz, was used to measure and register signals from pressure sensors, current sensors, voltage sensors, etc.

The equipment of the test stands ensured multiple measurements of sensor readings in each of the modes, which reduced the random error.

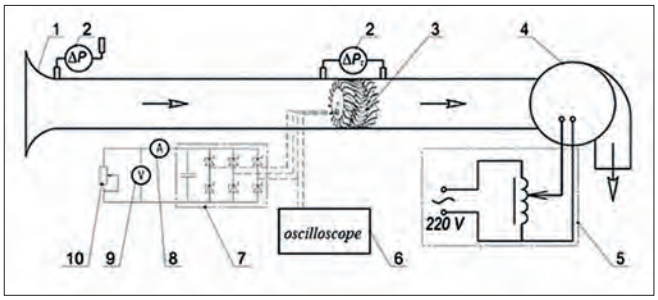


*Fig. 3. Diagram of the experimental stand for the study of the hydraulic resistance of the bidirectional turbine: 1 – lemniscate; 2 – inclined differential pressure gauge; 3 – turbine; 4 – fan; 5 – LATR; 6 – DAS oscilloscope SDS 1074CFL; 7 – diode bridge; 8 – ammeter; 9 – voltmeter; 10 – resistors*

The polling frequency of the pressure sensor controller by the STM32F407VGT6 controller was 10 kHz, and the bit rate was 32 bits.

A digital 4-channel oscilloscope, SDS 1074CFL, was used for the visual control of the operation of the TAE and the progression of the experiments, as a duplicating the measurement and registration of research information. Communication with the DAS and the oscilloscope was ensured using the USB interface. This microprocessor-based control and measurement system is discussed in more detail in [25].

An important task of the experimental research was to assess the operability of a model sample of a pulsed bidirectional turbine and its suitability for further experiments. All failings that were identified at the preparation stage were fixed.

Taking into account instrument errors and errors of approximation of expressions, the total measurement error does not exceed 2.5%. The error of determining the power of the generator, when using the existing DAS, does not exceed 2%.

## EXPERIMENT RESULTS

At this stage of the experiments, the characteristics of the turbogenerator exclusively in the longitudinal flow at different air flows rates were studied. The results of the experiments, that is, the pressure drops of the bidirectional turbine, are shown in Fig. 4.

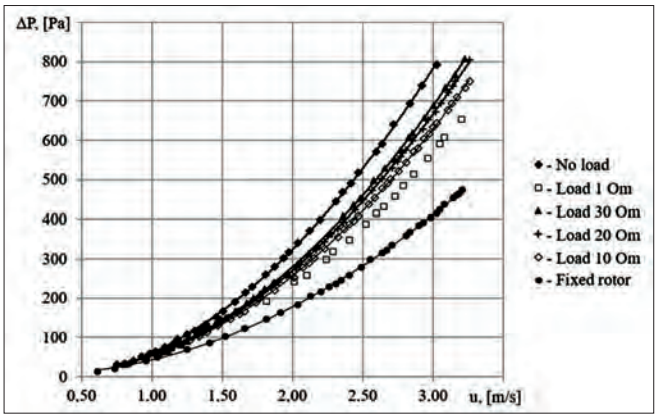


*Fig. 4. Dependence of hydraulic resistance of bidirectional turbines on flow velocity under different loads*

The load on the turbogenerator was changed using a set of precision resistors with different resistance values $R_i$. Data on the hydraulic resistance of a turbine with a fixed rotor were also obtained.

Research results have shown that a turbine with a fixed rotor has minimal flow resistance, which is quite natural. For a turbine with a free rotor, as the load decreases, the flow resistance increases. Furthermore, the data of these studies were used to verify the correctness of the results of the CFD modelling. The results of measuring the frequency of rotation of the turbine rotor depending on the speed of the oncoming flow are shown in Fig. 5. The main task of these experiments was to test the performance of the turbine in long-term operating modes and to assess the stability of external indicators.

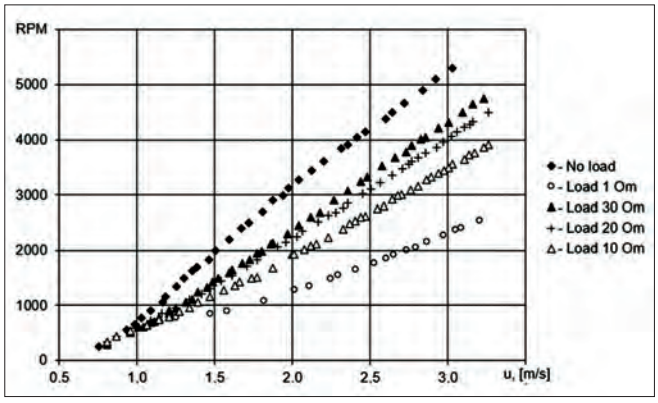


*Fig. 5. Turbine rotor revolutions depending on the speed of the oncoming flow*

It can be seen that the turbine rotation frequency also depends on the generator load. The maximum speed of rotation under the conditions of the experiment reached 5300 rpm. As can be expected, the maximum frequency of rotation of the turbine occurred when there was no load, in the idle regime. Additionally, during experimental studies, data were obtained that made it possible to determine its power depending on the speed of rotation. The results of these calculations are presented in Fig. 6.

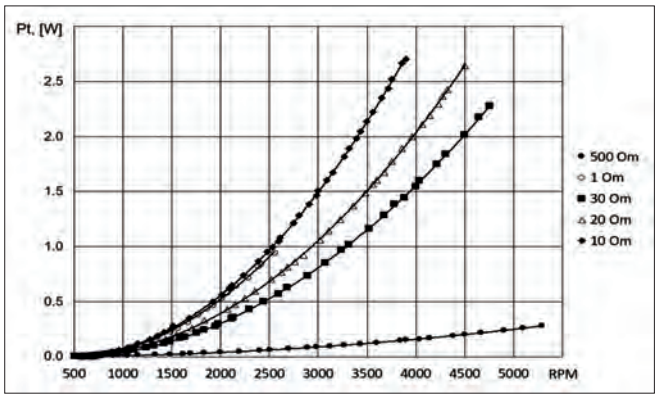


*Fig. 6. The electrical power generated by the experimental turbine generator at various rotor speeds and loads*

The minimum load mode of the generator was simulated using a resistor rated at 500 ohms. The results of the tests showed the suitability of the turbogenerator model for further research.

## CFD SIMULATION RESULTS

For a detailed study of hydrodynamic processes in the TAE resonator, a series of computational experiments was carried out. These studies were carried out with the help of various software products, which made it possible to compare the results obtained and assess the adequacy of the modelling.

In the ANSYS package [26], the channel geometry was created using the ANSYS Design Modeler and Blade Modeler programs, and the mesh was created using the ANSYS Turbo Grid program (Fig. 7); the analysis of the results was carried out using the CFD-Post software module. The features of various mathematical models that can be used in the CFD approach are described in detail in [27]–[31].

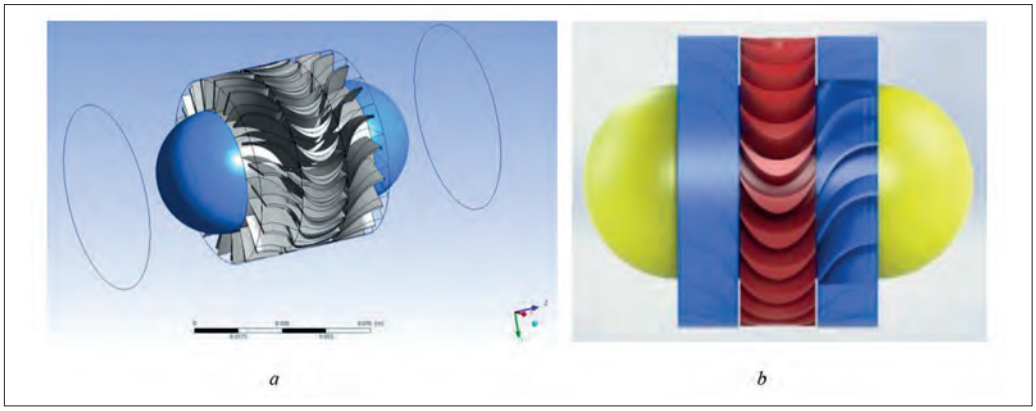


*Fig. 7. Experimental sample of a bidirectional turbine and its CFD model: a) ANSYS Design Modeler, b) SolidWorks 3D model*

In the first stage of research, in order to check the correctness of the construction of the CFD calculation models and create a time-efficient calculation scheme, test calculations were carried out. Considering the complexity of the task, the calculations were restricted to the fixed turbine rotor. In these experiments, the conditions of full-scale experiments to measure the resistance of a bidirectional turbine in a unidirectional flow were simulated.

The boundary conditions were set in accordance with the parameters of the physical experiment, and the standard k-e turbulence model was used. Fig. 8 shows the results of the CFD simulation of the hydraulic resistance of a resonator section with a bidirectional turbine.

It can be seen that the results of the CFD calculations and physical experiments coincide satisfactorily, since the difference between them does not exceed 10%. The existing deviations in the results can be explained by the difficulty of determining and taking into account the roughness of the surface of the bidirectional turbines and by some design deviations that were due to the capabilities of the existing 3D printer.

In further calculations, the hydrodynamic structure of the flow in the resonator with bidirectional turbines was studied. The calculations were made for the speed range of 3–25 m/s, which fully covers the range of amplitude values of the oscillating velocity that could be achieved during the experiments. The complexity of the hydrodynamic picture is shown in Figs. 9–11.

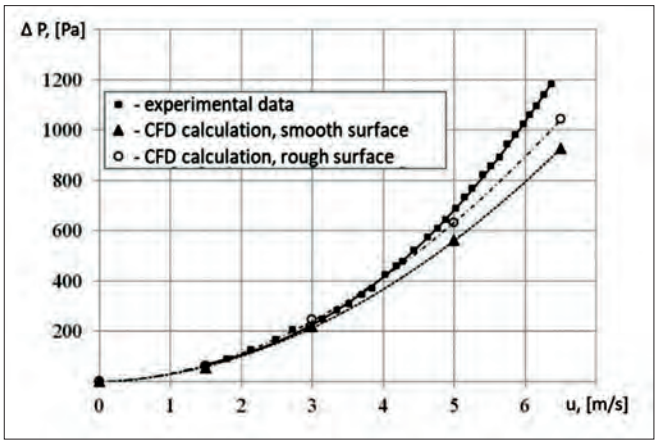


*Fig. 8. Hydraulic resistance of IDT specimen: comparison of experimental data with CFD simulation results*

The vortex structures in the flow behind the bidirectional turbines are more effectively visualised through the results presented in Figs. 12 and 13.

These figures demonstrate that within the resonator of the thermoacoustic generator, swirl flows developed, wherein the tangential velocity component equals nearly 60% of the longitudinal component. These persistent circulating vortex structures possess substantial energy accumulation capabilities and are rather stable.

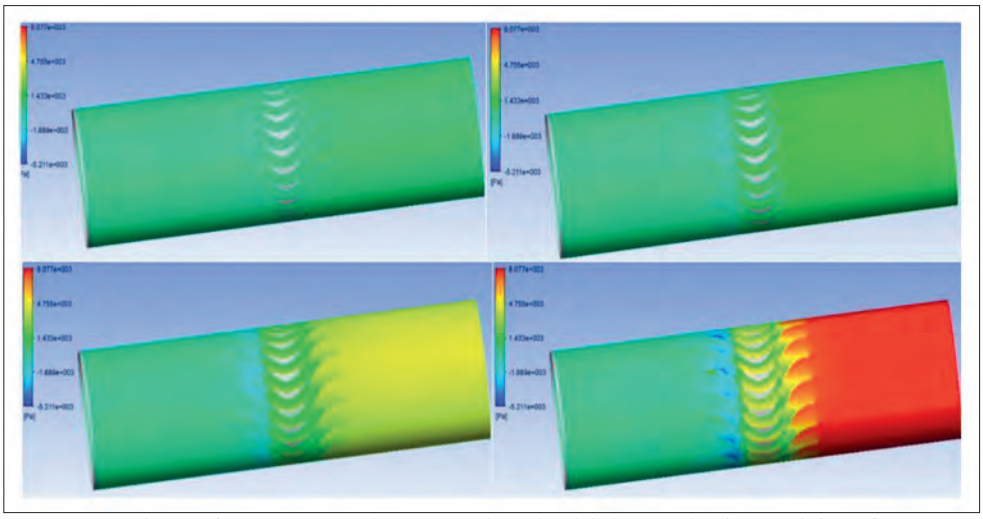

*Fig. 9. Distribution of static pressure in the resonator channel with bidirectional turbines at different flow rates*

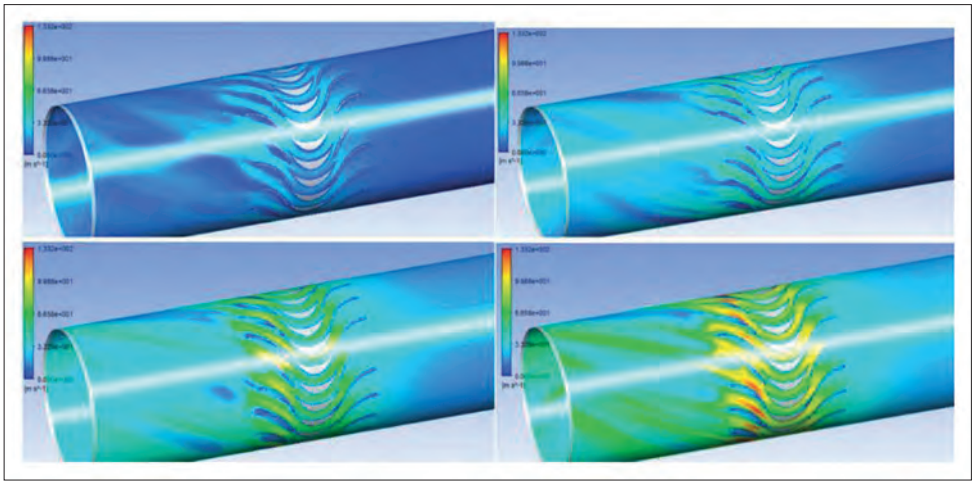

*Fig. 10. Distribution of static pressure in the resonator channel with bidirectional turbines at different flow rates*

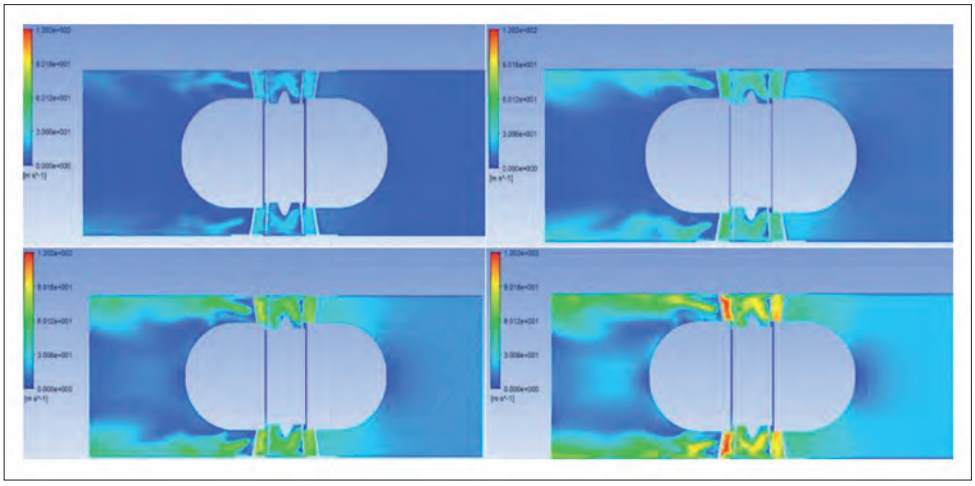

*Fig. 11. Velocity distribution across the resonator cross-section*

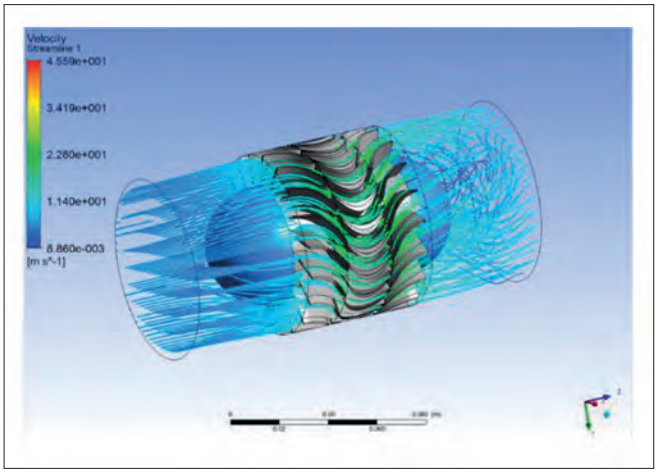


*Fig. 12. Current lines in a resonator with an experimental turbine; the rotor is stationary*

It can be argued that these phenomena in conditions of oscillating motion should lead to a non-uniform flow distribution in front of the straightening blades of bidirectional turbines, which is an undesirable factor. When designing such bidirectional turbines, measures should be taken to reduce these effects. In addition, the presence of tangential currents on the concave surface of the resonator will lead to the formation of secondary vortex structures of the Hertler-Taylor type, which also represent an energy-consuming mechanism.

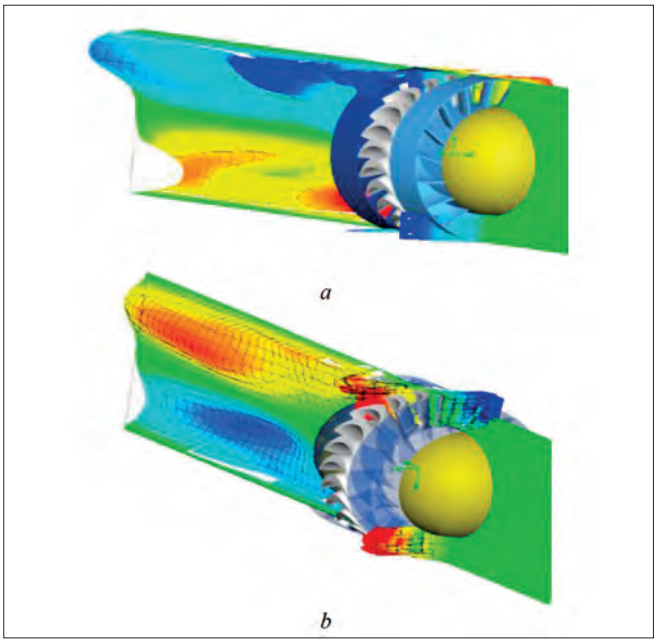


*Fig. 13. Distribution of circumferential velocity along the length of the resonator with bidirectional turbines: a) velocity of 5 m/s; b) velocity of 10 m/s*

## CONCLUSIONS

To perform the research program, a suitable experimental setup was developed; it includes a test worktable and a microprocessor data acquisition and recording system. A prototype of a turbogenerator equipped with a pulsed bidirectional turbine was fabricated, and a numerical counterpart was established for CFD simulations.

First, experimental evaluations were conducted under straight-line medium movement conditions with varying generator loads. Hydraulic resistance measurements of the turbine model within the resonator were sourced empirically. The results demonstrated that peak pressure losses transpire during the idling phase at the generator's minimal load. Under such conditions, rotor rotational speeds reached up to 5500 rpm.

A CFD framework was constructed to represent the combination of a bidirectional turbine and a thermoacoustic engine resonator. This model facilitated the exploration of turbine characteristics both for a stationary rotor and during the rotor's rotation.

The hydraulic resistance computations for the stationary-rotor turbine aligned closely with empirical results, deviating by less than 10%. This concurrence validates the utility of the developed CFD model for subsequent investigations. Simulations, executed across various software packages, consistently yielded analogous outcomes.

Numerical analyses revealed the emergence of pronounced tangential and radial secondary currents immediately behind the bidirectional turbine within the resonator. These secondary vortex patterns introduce augmented energy expenditures and require minimisation. Given the derived results, optimising the design of the bidirectional turbine's guide apparatus, as well as refining the profiling of the shroud and the resonator, emerges as a reasonable solution.

In analysing the current results, it is very important to consider that the simulations were focused on a small two-way turbine with an output power of only a few watts. However, for shipboard thermoacoustic WHRSs, the turbine generators should provide power at levels of approximately $10^2$ to $10^3$ kW. For such significantly larger structures, the occurrence of so-called large-scale effects is likely. In addition, the question of the construction of TATG resonators and their overall aggregate location is open.

In future efforts, the priority should be the integration of innovative design solutions aimed at mitigating the appearance of secondary radial flows in the resonators of high-power thermoacoustic generators.

## REFERENCES


1. N. Olmer, B. Comer, B. Roy, X. Mao, and D. Rutherford, "Greenhouse gas emissions from global shipping." [Online]. Available: https://theicct.org/wp-content/uploads/2021/06/Global-shipping-GHG-emissions-2013-2015_ICCT-Report_17102017_vF.pdf. [Accessed: Oct. 15, 2023].
2. International Maritime Organization, "Initial IMO GHG strategy." [Online]. Available: https://www.imo.org/en/MediaCentre/HotTopics/Pages/Reducing-greenhouse-gas-emissions-from-ships.aspx. [Accessed: Oct. 15, 2023].
3. International Maritime Organization, "Note by the International Maritime Organization to the UNFCCC Talanoa Dialogue." [Online]. Available: https://unfccc.int/sites/default/files/resource/250_ IMO%20submission_Talanoa%20Dialogue_April%202018.pdf. [Accessed: Oct. 15, 2023].
4. International Maritime Organization, "IMO. Low carbon shipping and air pollution control." [Online]. Available: http://www.imo.org/en/MediaCentre/HotTopics/GHG/Pages/default.aspx. [Accessed: Oct. 15, 2023].
5. International Maritime Organization, "Fourth IMO GHG study 2020 executive-summary." [Online]. Available: https://wwwcdn.imo.org/localresources/en/OurWork/Environment/Documents/ Fourth%20IMO%20GHG%20Study%202020%20Executive-Summary.pdf. [Accessed: Oct. 15, 2023].
6. Finnish Marine Industries, "Journey to a carbon-free world: Introducing the NYK SUPER ECO SHIP 2050." [Online]. Available: https://meriteollisuus.teknologiateollisuus.fi/en / ajankohtaista/news/journey-carbon-free-world-introducing-nyk-super-eco-ship-2050. [Accessed: Oct. 15, 2023].
7. H. Shi, Q. Zhang, M. Liu, K. Yang, and J. Yuan, "Numerical Study of the Ejection Cooling Mechanism of Ventilation for a Marine Gas Turbine Enclosure," *Polish Maritime Research*, Vol. 29, No. 3, pp. 119–127, 2022, doi: org/10.2478/pomr-2022-0032.
8. T. Niksa-Rynkiewicz, A. Witkowska, J. Głuch, and M. Adamowicz, "Monitoring the Gas Turbine Start-Up Phase on a Platform Using a Hierarchical Model Based on Multi-Layer Perceptron Networks," *Polish Maritime Research*, Vol. 29, No. 4, pp. 123–131, 2022, doi: 10.2478/pomr-2022-0050.
9. E.-L. Tsougranis and D. Wu, "A feasibility study of organic Rankine cycle (ORC) power generation using thermal and cryogenic waste energy on board an LNG passenger vessel," *International Journal of Energy Research*, Vol. 42, No. 9, pp. 3121–3142, July 2018, doi: 10.1002/er.4047.
10. M. E. Mondejar, J. G. Andreasen, L. Pierobon, U. Larsen, M. Thern, and F. Haglind, "A review of the use of organic Rankine cycle power systems for maritime applications," *Renewable and Sustainable Energy Reviews*, Vol. 91, pp. 126–151, 2018, doi: 10.1016/j.rser.2018.03.074.
11. T. Hoang, "Waste heat recovery from diesel engines based on Organic Rankine Cycle," *Applied Energy*, Vol. 231. 2018, doi: 10.1016/j.apenergy.2018.09.022.

12. O. Cherednichenko, S. Serbin, and M. Dzida, "Application of thermo-chemical technologies for conversion of associated gas in diesel-gas turbine installations for oil and gas floating units," *Polish Maritime Research*, Vol. 26, No. 3, pp. 181–187, Sep. 2019, doi: 10.2478/pomr-2019-0059.

13. G. W. Swift, "Thermoacoustic engines," *J. Acoust. Soc. Am.*, Vol. 84, No. 4, pp. 1145–1180, 1988.

14. G. W. Swift, "Thermoacoustics: A unifying perspective for some engines and refrigerators," *Acoust. Soc. Am.*, 2002. ISBN 0-7354-0065-2.

15. L. M. Qi, P. Lou, K. Wang, et al., "Characteristics of onset and damping in a standing-wave thermoacoustic engine driven by liquid nitrogen," *Chin. Sci. Bull.*, Vol. 58, pp. 1325-1330, 2013, doi: 10.1007/s11434-012-5214-z.

16. Z. Yang, V. Korobko, M. Radchenko, and R. Radchenko, "Improving thermoacoustic low-temperature heat recovery systems," *Sustainability (Switzerland)*, Vol. 14, No. 19, art. No. 12306, 2022, doi: 10.3390/su141912306.

17. T. K. Das, P. Halder, and A. Samad, "Optimal design of air turbines for oscillating water column wave energy systems: A review," *Int. J. Ocean Clim. Syst.*, Vol. 8, No. 1, pp. 37–49, 2017, doi: 10.1177/1759313117693639.

18. A. F. O. Falcao and J. C. C. Henriques, "Oscillating-water-column wave energy converters and air turbines: A review," Renewable Energy, 2015, doi: 10.1016/j.renene.2015.07.086.

19. A. Thakker and F. Hourigan, "Modeling and scaling of the impulse turbine for wave power applications," Renewable Energy, Vol. 29, No. 3, pp. 305–317, 2004, doi: 10.1016/S0960-1481(03)00253-2.

20. D. Liu, Y. Chen, W. Dai, et al., "Acoustic characteristics of bi-directional turbines for thermoacoustic generators," *Front. Energy*, Vol. 16, pp. 1027–1036, 2022, doi: 10.1007/s11708-020-0702-3.

21. M. A. Elhawary, A. H. Ibrahim, A. S. Sabry, and E. Abdel-Rahman, "Experimental study of a small scale bi-directional axial impulse turbine for acoustic-to-mechanical power conversion," *Renewable Energy*, 2020, doi: 10.1016/j.renene.2020.05.162.

22. C. Iniesta, J. L. Olazagoitia, J. Vinolas, and J. Aranceta, "Review of travelling-wave thermoacoustic electric-generator technology," in *Proceedings of the Institution of Mechanical Engineers, Part A: Journal of Power and Energy*, 2018, doi: 10.1177/0957650918760627.

23. Y. Kondratenko, S. Serbin, V. Korobko, and O. Korobko, "Optimisation of bi-directional pulse turbine for waste heat utilization plant based on green IT paradigm," *Studies in Systems, Decision and Control*, Vol. 171, pp. 469–485, 2019, doi: 10.1007/978-3-030-00253-4_20.

24. T. Kloprogge, "Turbine design for thermo-acoustic generator," Master's thesis, Aeronautical Engineering, Hogeschool. Holland Delft, 2012. Available: https://bioenergyforumfact.org/sites/default/files/2018-06/5.%20Turbine%20 Design%20for%20a%20Thermo-acoustic%20Generator.pdf. [Accessed: Oct. 15, 2023].

25. Y. Kondratenko, O. Korobko, and V. Korobko, "Microprocessor system for thermoacoustic plants efficiency analysis based on a two-sensor method," *Sensors & Transducers*, Vol. 24, Aug. 2013. Available: https://www.academia.edu/95466184/Microprocessor_System_for_Thermoacoustic_Plants_Efficiency_Analysis_Based_on_a_Two_Sensor_Method. [Accessed: Oct. 15, 2023].

26. ANSYS, Inc., ANSYS *Fluent Theory Guide.* ANSYS, Inc., 2013.

27. S. I. Serbin, I. B. Matveev, and G. B. Mostipanenko, "Plasma-assisted reforming of natural gas for GTL: Part II - Modeling of the methane-oxygen reformer," *IEEE Trans. Plasma Sci.*, Vol. 43, No. 12, pp. 3964–3968, 2015, doi: 10.1109/TPS.2015.2438174.

28. I. Matveev, S. Serbin, T. Butcher, and N. K. Tutu, "Flow structure investigations in a Tornado combustor," in *4th International Energy Conversion Engineering Conference, AIAA2006-4141*, Vol. 2, 2006, pp. 1001–1013, doi: 10.2514/6.2006-4141.

29. O. Cherednichenko, S. Serbin, and M. Dzida, "Investigation of the combustion processes in the gas turbine module of an FPSO operating on associated gas conversion products," *Polish Maritime Research*, Vol. 26, No. 4, pp. 149–156, 2020, doi: 10.2478/pomr-2019-0077.

30. S. Serbin, K. Burunsuz, M. Dzida, J. Kowalski, and D. Chen, "Investigation of ecological parameters of a gas turbine combustion chamber with steam injection for the floating production, storage, and offloading vessel," *International Journal of Energy and Environmental Engineering*, Vol. 13, No. 3, pp. 873–888, 2022, doi: 10.1007/s40095-021-00433-w.

31. I. B. Matveev, N. V. Washchilenko, and S.I. Serbin, "Plasma-Assisted Reforming of Natural Gas for GTL: Part III - Gas Turbine Integrated GTL," *IEEE Trans. Plasma Sci.*, Vol. 43, No. 12, pp. 3969–3973, 2015, doi: /10.1109/TPS.2015.2464236.